

Platinum-Ruthenium Nanoparticles: Active and Selective Catalysts for Hydrogenation of Phenylacetylene

Jan-Yves Ruzicka,^A David P. Anderson,^A Sally Gaw,^A
and Vladimir B. Golovko^{A,B,C}

^ADepartment of Chemistry, University of Canterbury, Private Bag 4800,
Christchurch 8140, New Zealand.

^BThe MacDiarmid Institute for Advanced Materials and Nanotechnology,
Wellington 6140, New Zealand.

^CCorresponding author. Email: vladimir.golovko@canterbury.ac.nz

Bimetallic metal nanoparticles are often more catalytically active than their monometallic counterparts, due to a so-called 'synergistic effect'. Atomically precise ruthenium-platinum clusters have been shown to be active in the hydrogenation of phenylacetylene to styrene (a reaction of importance to the polymer industry). However, the synthesis of these clusters is generally complex, and cannot be modified to produce clusters with differing metal compositions or ratios. Hence, any truly systematic study of compositional effects using such clusters is hindered by the inaccessibility of certain metal ratios. In this study, a series of larger bimetallic ruthenium-platinum colloids of varying metal ratios was synthesised in solution and immobilised on silica. Catalytic activity was evaluated by hydrogenation of phenylacetylene to styrene. Both bimetallic and monometallic colloids were active catalysts for the hydrogenation of phenylacetylene to styrene and further to ethylbenzene. Of those studied, a catalyst composed of 73 % platinum-27 % ruthenium (by moles) showed the highest activity. This suggests that synergistic effects play an important role in the catalysis of this reaction. To our knowledge this is the first systematic study of ruthenium-platinum nanoparticle catalytic activity on this reaction.

Manuscript received: 27 April 2012.

Manuscript accepted: 4 June 2012.

Published online: 3 July 2012.

Introduction

Nanoparticles display chemical and physical properties that differ from their bulk phase counterparts. This difference can be explained by electronic and surface structure effects originating from their size.^[1,2] These properties, coupled with their large surface-to-volume ratios, make nanoparticles ideal candidates as catalysts for a variety of reactions, such that the majority of modern heterogeneous catalysts are composed of nanoparticles.^[2] The group ten transition metals in particular are well known as active catalysts in various hydrogenation reactions. Nanoparticles containing palladium or platinum, for example, have been documented as catalysts for the selective hydrogenation of alkenes and polyenes, even in aromatic systems.^[3,4]

It has previously been shown that bimetallic nanoparticles may display an activity greater than physical mixtures of the relevant monometallic nanoparticles in the same ratio.^[5] This phenomenon has been dubbed the synergistic effect. For example, Bönemann and co-workers have reported^[6] that Rh-Pt alloy nanoparticles outperform a simple physical mixture of Rh and Pt monometallic nanoparticles in the hydrogenation of crotonic acid to butanoic acid, while Hogarth has shown that Pt-Ru nanoparticles are also effective catalysts for the combustion of methanol.^[7] It is thought that ruthenium surface sites contribute to methanol combustion by removing CO groups that would otherwise poison the platinum active site. This is an example of how synergistic effects (here, the presence of a

heteroatom active site) may improve the activity of bimetallic catalysts.

Styrene is an industrially and commercially valuable material. The most common use of styrene is as a feedstock in the production of polystyrene, one of the least expensive thermoplastic polymers available on a cost-per-volume basis.^[8]

Styrene is generally synthesised by the dehydrogenation of ethylbenzene. However, this process may also produce phenylacetylene in appreciable quantities. The hydrogenation (to ethylbenzene) or semi-hydrogenation (to styrene) of phenylacetylene in styrene feedstocks is of considerable industrial importance, as the presence of phenylacetylene has been shown to poison polymerisation catalysts.^[8]

Platinum and ruthenium monometallic nanoparticles have already been explored as catalysts for the semi-hydrogenation of phenylacetylene.^[9] Platinum-based catalysts demonstrate a greater activity towards hydrogenation of phenylacetylene, while ruthenium nanoparticle catalysts are reported to be more selective in the production of styrene (~98 % selectivity). While ruthenium-based catalysts are more selective, they display lower overall activity.

Adams and co-workers^[10] have explored the activity of small, precisely-defined ruthenium-platinum metal clusters for the hydrogenation of phenylacetylene. These clusters have been shown to be active towards production of styrene, but are complex and time-consuming to synthesise, especially

compared with contemporary ‘one-pot’ methods used in the synthesis of larger metal colloids.

To our knowledge, no study has been performed on the activity of colloidal bimetallic ruthenium-platinum nanoparticles towards hydrogenation of phenylacetylene. For this reason we have systematically explored the activity and selectivity of a series of support-immobilised bimetallic ruthenium-platinum nanoparticles towards this reaction. The particles were synthesised using a simple one-pot sol-gel approach, which allows synthesis of bimetallic Pt-Ru systems with constant (~ 2 nm) particle sizes across a wide range of chemical compositions.^[11,12]

Results and Discussion

In this study, a series of bimetallic platinum-ruthenium nanoparticles was synthesised by reduction in solution (as previously reported in literature) and immobilised on silica. Nanoparticle size was determined by transmission electron microscopy, and metal composition and loading were determined by inductively-coupled plasma mass-spectrometry (ICP-MS). Both particle size and metal composition data agreed with those shown in literature. These immobilised nanoparticles were then used as catalysts in the hydrogenation of phenylacetylene to styrene and ethyl benzene.

Synthesis

A series of bimetallic platinum-ruthenium nanoparticles were synthesised by reduction of RuCl_3 and H_2PtCl_6 precursors in methanol using polyvinyl pyrrolidone (PVP) as a capping agent to control growth. This has been previously shown to produce a relatively monodisperse colloid of bimetallic nanoparticles.^[11] The metal composition of the nanoparticles was controlled by variation of the concentration of the metal precursors. A series of catalysts with platinum molar compositions of 10% (Pt10) through 100% (Pt100) were produced.

These nanoparticles were immobilised on silica support (1% loading by mass). These materials were then calcined under vacuum before being washed with methanol to remove excess PVP and any non-immobilised nanoparticles.

Characterisation

The resultant support-immobilised catalysts were characterised by inductively-coupled plasma mass spectrometry (ICP-MS) to determine both metal loading and actual platinum-ruthenium ratio (Fig. 1). From these results it can be seen that the measured metal ratio is generally consistent with what is expected, however there is some variation between nominal (target) and actual (measured by ICP-MS) metal ratio. Generally the platinum content is higher than predicted. A similar discrepancy for an analogous Ru-Pt colloid system has been reported previously,^[13] and could be due to a greater binding affinity of PVP for platinum than ruthenium.^[11] It can also be seen that the actual metal loading on silica varies considerably across different catalysts, generally between 0.4% and 0.8%. This indicates that the nanoparticle-support binding process does not guarantee complete immobilisation of particles on support. Of note, it appears that ruthenium-rich particles are immobilised less efficiently than platinum-rich particles. This behaviour may also contribute to the relatively high platinum content in reported catalysts.

Transmission electron microscopy (Philips 200 keV TEM) was used to characterise the morphology of the Pt50, Pt70, and

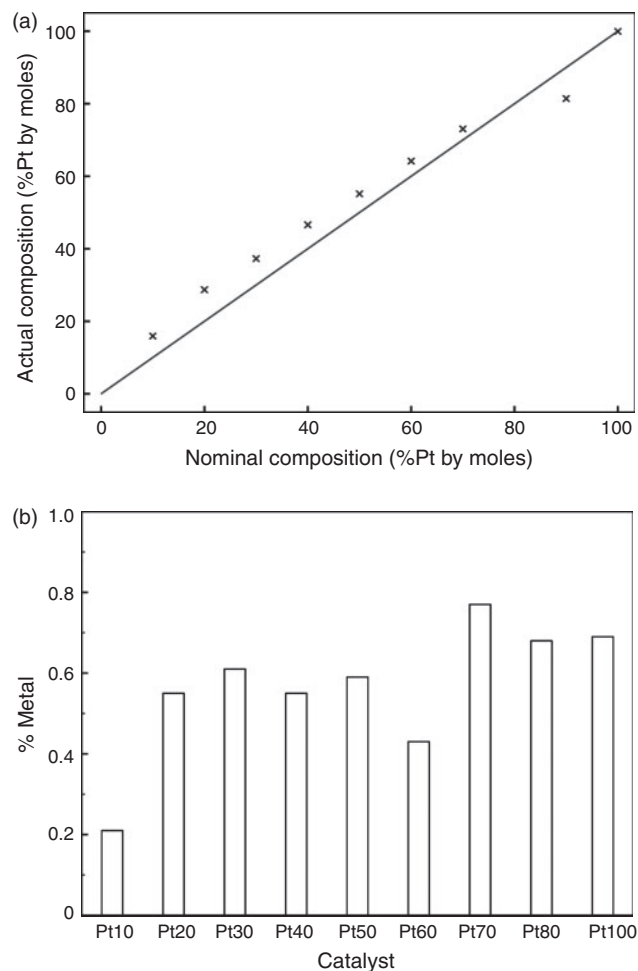


Fig. 1. Catalyst composition varied from planned metal ratios and loadings. (a) Actual metal ratio for each catalyst; (b) total metal loading. Line in Fig. 1a indicates ideal metal composition.

Pt100 systems after calcination. TEM analysis of the above samples showed particles of diameter around 2 nm ($\text{Pt50} = 2.3 \pm 0.5$ nm; $\text{Pt70} = 3.0 \pm 0.9$ nm; $\text{Pt100} = 2.0 \pm 0.6$ nm) for all samples (Fig. 2). Obtained data is in agreement with previously-reported characterisation of Pt and Pt-Ru nanoparticles synthesised using methods similar to ours.^[11,12] Very occasional aggregation was noted on the silica support, however powder X-ray diffraction (PXRD) analysis of the sample showed no crystalline peaks. This indicates that while aggregation during calcination may have occurred, the majority of the catalyst still consists of small (~ 2 nm), well dispersed particles that do not give rise to PXRD peaks due to Scherrer broadening.

In addition, high-resolution TEM (HRTEM) images of the nanoparticles showed fringing in both monometallic and bimetallic particles, indicating a high degree of crystallinity (Fig. 3). Fringing patterns were analysed by Fourier transform of HRTEM images. While fringing patterns observed did not coincide with either documented platinum or ruthenium fringing patterns, this may be attributable to lattice deformation due to the small size of the particles.^[14] Of particular note, the fringing pattern increased linearly with increasing platinum concentration over the observed range. This is likely due to Vegard's Law,^[15] and indicates the formation of bimetallic ruthenium-platinum alloy rather than a simple physical mixture of metal nanoparticles.

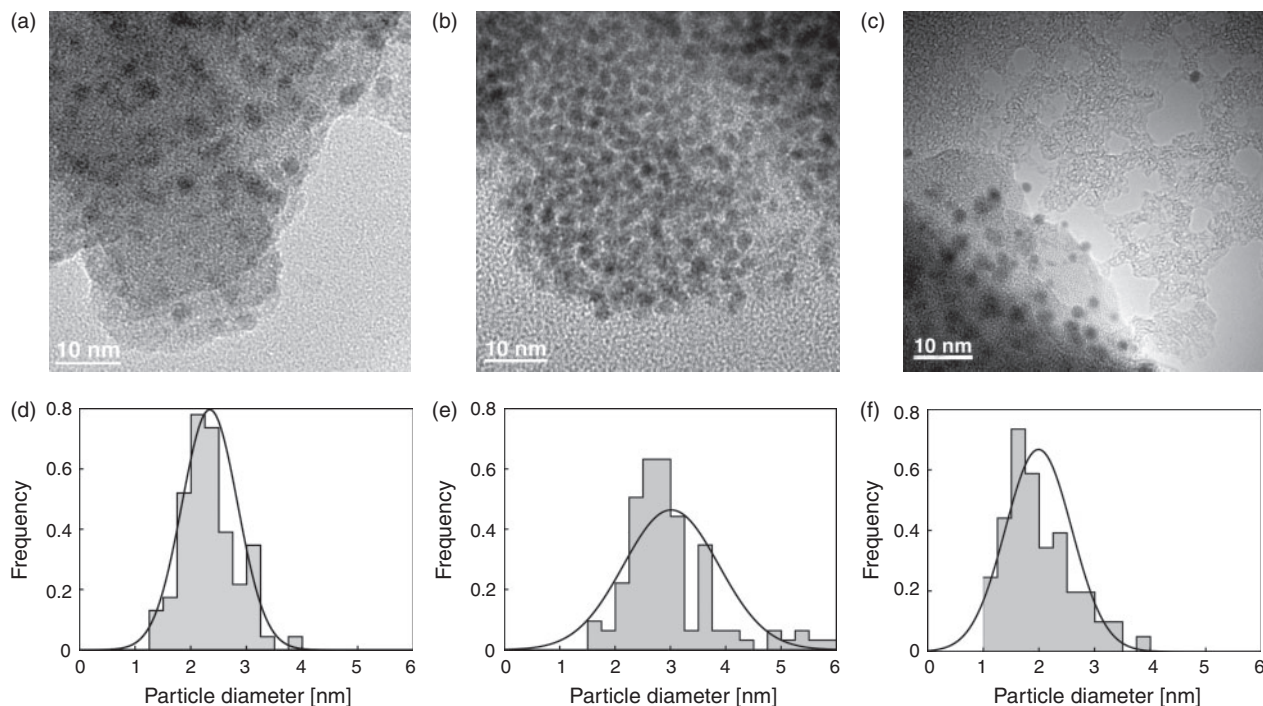


Fig. 2. TEM images of (a) Pt50, (b) Pt70, and (c) Pt100 catalysts immobilized on silica support, and particle sizing data for (d) Pt50 ($\mu = 2.3$, $\sigma = 0.5$), (e) Pt70 ($\mu = 3.0$, $\sigma = 0.9$), and (f) Pt100 ($\mu = 2.0$, $\sigma = 0.6$). The Gaussian curve shows calculated normal distribution from raw data.

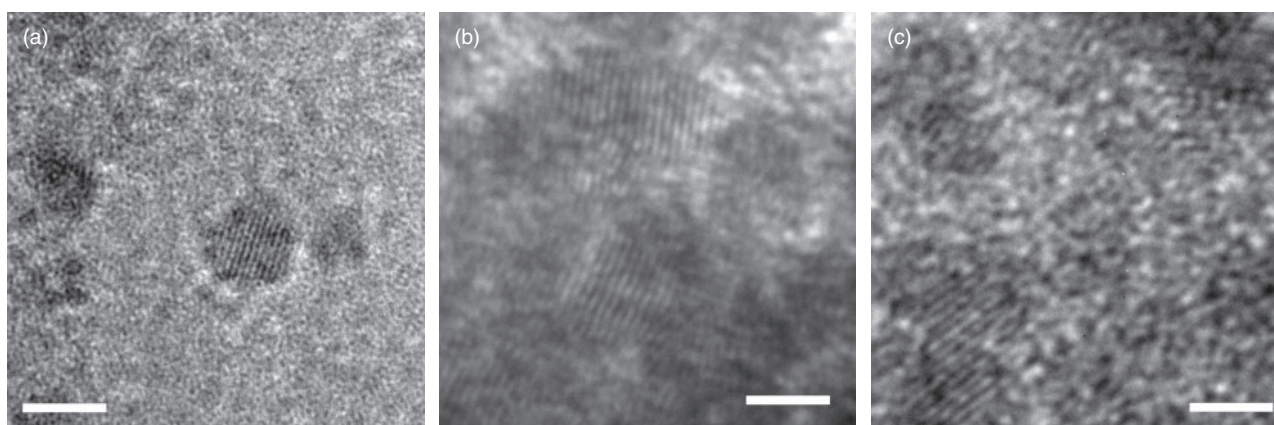


Fig. 3. HRTEM of (a) Pt50, (b) Pt70, and (c) Pt100 showing fringing. Scale bar length is 2 nm.

Catalytic Activity

The performance (activity and selectivity, Table 1) of our catalysts was tested in a model reaction: the hydrogenation of phenylacetylene to styrene (Scheme 1). The reaction was performed in a Teflon-lined stainless steel pressurised reactor (Parr) under ~ 10 bar of hydrogen at 40°C for one hour. The reaction product mixtures were centrifuged to remove the catalyst and the supernatant was analysed by gas chromatography. Chromatograms showed peaks due to phenylacetylene, styrene, and ethyl benzene (quantified against a series of standard solutions), as well as the solvent (methanol) and the internal standard (decane). No other peaks were observed.

The activity of each catalyst, adjusted for both total (Pt + Ru) metal loading on each catalyst, and the amount of catalyst used in each catalytic test, is presented in Fig. 4.

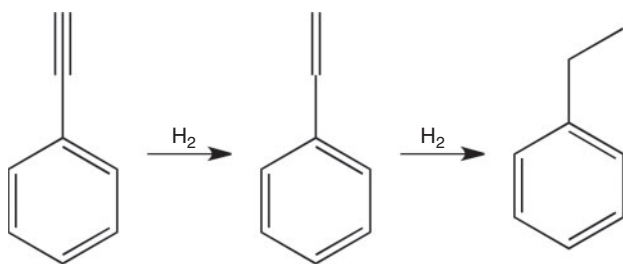
Fig. 5 shows the activity of each catalyst as a function of the molar amount of each specific metal present (adjusted for metal

Table 1. Hydrogenation of phenylacetylene (PA) over the PtRu-silica system

Catalyst	%Pt	Avg. rate ^A	Selectivity	
			EB [%] ^B	Styrene [%]
Pt10	15.92	0.39	8.5	91.5
Pt20	28.71	1.09	18.3	81.7
Pt30	37.27	1.48	19.4	80.1
Pt40	46.60	1.58	15.8	84.2
Pt50	55.15	1.75	14.8	85.2
Pt60	64.18	1.41	12.7	87.3
Pt70	73.04	3.20	16.0	84.0
Pt80	81.42	1.87	13.4	86.6
Pt100	99.94	2.34	11.2	88.8

^AAverage rate given in units of (mol of PA)/(mol of catalyst · h).

^BEthyl benzene.



Scheme 1. Hydrogenation of phenylacetylene to styrene and ethylbenzene.

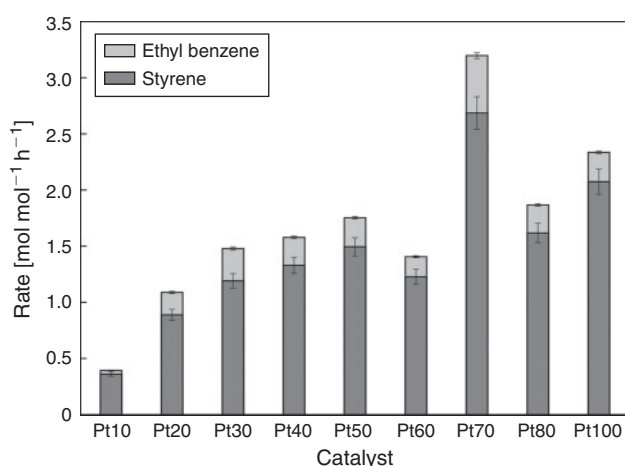


Fig. 4. Catalyst activity, normalised for moles of metal and time. The activity is measured as the number of moles of the reactant phenylacetylene converted per mole of catalyst per hour of reaction. (Error bars show estimated experimental error.)

loading and amount of catalyst used). There is a very significant ($r = 0.812$; $p < 0.01$, Pearson's correlation) correlation between catalytic activity and platinum content (shown as a solid line in Fig. 5a). Fig. 5b also demonstrates that a similar correlation is not observed between ruthenium content.

Despite the general correlation between amount of platinum and catalytic activity, the most active catalyst observed is Pt70, with an actual (measured) platinum content of 73 % (by moles). This may indicate that there is some synergistic effect between the platinum and ruthenium that enhances the activity of Pt-Ru nanoparticles of this particular molar ratio (Pt : Ru \approx 84 : 16 by mass, 73 : 27 by moles) to the hydrogenation of styrene.

In order to confirm that the particles observed were indeed bimetallic, and not a physical mixture of monometallic particles, TEM-energy dispersive X-ray spectroscopy (TEM-EDS) was performed on the Pt70 (73 % Pt) sample. The change in metal ratio between EDS measurements at low magnification ($\approx 8500\times$) and high magnification (up to $265000\times$) was very small ($\sigma = 3\%$ for all measurements). If the catalyst were composed of a physical mixture of monometallic particles, the metal ratio should change at high magnification as the number of particles analysed decreases. This phenomenon was observed at several sites on the catalyst, confirming that it is indeed bimetallic.

These findings build on top of previous reports on the use of several atomically-precise metal clusters in catalysis.^[16,17] In contrast to these reports, we have screened a wide range of

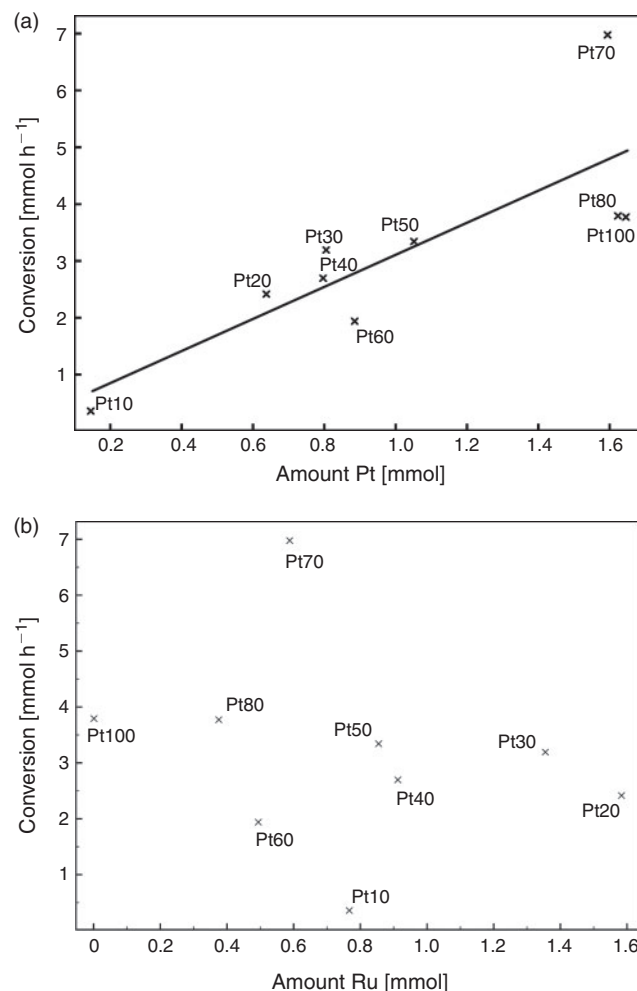


Fig. 5. Conversion of each catalyst (measured in mmol of phenylacetylene lost per hour) as a function of metal loading (in mmol) for (a) platinum and (b) ruthenium. A strong ($r = 0.812$) linear correlation is seen between platinum metal loading and conversion of phenylacetylene.

catalysts based on support-immobilised nanoparticles of similar sizes (thus excluding variations in activity due to size effects) with chemical compositions varying systematically and considerably across the series. Such a goal is often difficult to achieve in the case of cluster-based catalysts.

Conclusion

The aims of this research were: first, to synthesise a range of bimetallic ruthenium-platinum colloids, and second, to determine their catalytic activity in the hydrogenation of phenylacetylene.

Analysis by ICP-MS showed that while metal loading was consistently lower than expected, the platinum-ruthenium ratio of each catalyst was generally consistent with the expected value, albeit with a systematically higher platinum ratio than expected. TEM analysis of the catalysts showed that supported metal nanoparticles were ~ 2 nm in size, indicating that no particle aggregation had taken place during catalyst fabrication and activation.

Hydrogenation of phenylacetylene using the synthesised catalysts resulted in a mixture of styrene and ethyl benzene, with a selectivity towards styrene of 80–90 % across the range of

Pt:Ru ratios studied. Overall, catalytic activity appears to depend directly on the amount of platinum in the catalyst. The most active catalyst was found to be composed of 84 % platinum by mass (73 % by moles), which may be indicative of a synergistic effect between the platinum and ruthenium at this particular ratio.

ICP-MS results showed that an appreciable amount of colloid was not properly immobilised on the surface of the silica support, causing metal loading to vary appreciably. Further work should aim to optimise the method of catalyst immobilisation, minimising the loss of metal colloid. In addition, there has not yet been a comprehensive attempt to elucidate the mechanism of phenylacetylene hydrogenation on the surface of the metal catalyst. A better understanding of how the reactant molecule interacts with the catalyst surface, based on careful modelling, may also be key to understanding exactly how any synergistic effect alters the reaction rate.

Experimental

Materials

H₂PtCl₆·6H₂O (BDH), RuCl₃ (Precious Metals Online), PVP (MW ≈ 40000, Sigma-Aldrich), ethyl benzene (BDH), styrene (Merck), and phenylacetylene (Aldrich) were used as obtained. All solvents were analytical grade unless noted otherwise. Acids used for digestion were Merck Suprapur HNO₃ and Tracepur HCl.

Silica gel was obtained from Scharlau. It was recorded to have an overall particle size of 0.04–0.06 mm, a mean pore diameter of 60 Å, and a surface area of 500 m² g⁻¹.

Methanol used for catalysis was dried with iodine and magnesium.^[18]

Decane used as the internal standard was obtained from Sigma-Aldrich (>99 %).

Synthesis

Metal solutions were made by dissolving ruthenium or platinum precursor (RuCl₃ or H₂PtCl₆ respectively) in methanol to achieve a concentration of 2 × 10⁻³ mol L⁻¹. PVP was added to these solutions to a concentration of 4 × 10⁻² mol L⁻¹ (monomeric units).

Solutions containing 2 × 10⁻⁴ mol of metal were formed by combining various ratios of these two solutions at room temperature, and 1 × 10⁻³ mol of sodium borohydride (as solid) was added quickly to reduce the metal. The resulting colloid was stirred for one hour to ensure complete reduction and nanoparticle formation.

Immobilisation

The amount of silica used for each immobilisation was calculated to give a 1 % w/w metal loading, assuming complete reduction and immobilisation.

Silica was added to a colloidal solution in methanol and stirred for one hour. Methanol was removed by vacuum and the powder left was calcined for 2 h under vacuum at 200°C. After cooling to room temperature, methanol (100 mL) was added and the mixture stirred for a further 30 min to remove surfactants and any colloidal nanoparticles that had not been immobilised. Following overnight flocculation of the solid, the methanol wash was carefully removed by syringe, and the powder was dried under vacuum.

Characterisation

Nanoparticles were characterised by TEM using a Philips CM-200 transmission electron microscope. Samples were prepared by suspending activated catalyst in a small amount of methanol and delivering a small drop of the slurry onto a Cu 300 mesh TEM sample grid covered with a holey carbon film.

ICP-MS analyses were performed using an Agilent 7500cx equipped with an octopole collision cell (Agilent Technologies Inc., Tokyo, Japan). Each catalyst (100 mg) was first digested in a concentrated solution of hydrochloric and nitric acid (*aqua regia*) for 3 h at 80°C. This solution was made up to 50 mL and then diluted thirty times with dilute (6 %) *aqua regia*. 200 µL of this solution was withdrawn and made up to 6 mL with 6 % *aqua regia*. The resultant solution was analysed by ICP-MS for platinum and ruthenium.

Catalysis

Catalyst (50 mg) was added to 1 mL of phenylacetylene, 38.75 mL of dried methanol and 250 µL of decane internal standard in a 100 mL Teflon-lined Parr pressure reactor. This was heated to 40°C under argon with stirring of 1450 rpm. Once temperature was reached, the system was flushed with hydrogen before being pressurised with 10 bar of hydrogen gas. The pressure was monitored using a Parr 4842 pressure monitor. The reaction was allowed to proceed for one hour.

The reaction products were centrifuged to remove the catalyst. The supernatant was analysed using a Shimadzu GC-2010 gas chromatograph equipped with a Restek Rxi-5Sil MS column. Helium was used as a carrier gas, with a flow rate of 17.4 cm s⁻¹. The injection volume was 1 µL, the injection temperature was 200°C, the FID temperature was 300°C and the column was kept at 80°C.

A series of five standards of phenylacetylene, styrene, and ethylbenzene were prepared in methanol, with concentrations ranging from 1 mM through 500 mM. These standards were used to calibrate the GC, using the conditions described above.

Acknowledgements

The authors acknowledge the University of Canterbury and the MacDiarmid Institute for funding, as well as the help of Robert Stainthorpe with ICP-MS measurements.

References

- [1] G. A. Ozin, A. C. Arsenault, *Nanochemistry* **2006** (RSC Publishing: Dorchester).
- [2] A. T. Bell, *Science* **2003**, 299, 1688. doi:10.1126/SCIENCE.1083671
- [3] J. M. Thomas, B. F. G. Johnson, R. Raja, G. Sankar, P. A. Midgley, *Acc. Chem. Res.* **2003**, 36, 20. doi:10.1021/AR990017Q
- [4] A. B. Hungria, R. Raja, R. D. Adams, B. Captain, J. M. Thomas, P. A. Midgley, V. Golovko, B. F. G. Johnson, *Angew. Chem. Int. Edit.* **2006**, 45, 4782. doi:10.1002/ANIE.200600359
- [5] R. D. Adams, *J. Organomet. Chem.* **2000**, 600, 1. doi:10.1016/S0022-328X(00)00028-0
- [6] H. Bönnemann, R. M. Richards, *Eur. J. Inorg. Chem.* **2001**, 2455. doi:10.1002/1099-0682(200109)2001:10<2455::AID-EJIC2455>3.0.CO;2-Z
- [7] M. P. Hogarth, T. R. Ralph, *Platinum Met. Rev.* **2002**, 46, 146.
- [8] *Ullmann's Encyclopedia of Industrial Chemistry* **2006** (Ed. F. Ullmann) (John Wiley & Sons, Inc.: Hoboken, NJ).
- [9] J. Badano, C. Lederhos, M. Quiroga, P. L'Argentière, *Quim. Nova* **2010**, 33, 48. doi:10.1590/S0100-40422010000100010
- [10] R. D. Adams, B. Captain, L. Zhu, *J. Am. Chem. Soc.* **2004**, 126, 3042. doi:10.1021/JA049955Y

- [11] M. Liu, W. Yu, H. Liu, J. Zheng, *J. Colloid Interf. Sci.* **1999**, *214*, 231. doi:10.1006/JCIS.1999.6186
- [12] Y. Shimazaki, Y. Kobayashi, S. Yamada, T. Miwa, M. Konno, *J. Colloid Interf. Sci.* **2005**, *292*, 122. doi:10.1016/J.JCIS.2005.05.052
- [13] D. Nagao, Y. Shimazaki, Y. Kobayashi, M. Konno, *Colloid Surface A.* **2006**, *273*, 97. doi:10.1016/J.COLSURFA.2005.08.011
- [14] R. Schlögl, S. B. Abd Hamid, *Angew. Chem. Int. Edit.* **2004**, *43*, 1628. doi:10.1002/ANIE.200301684
- [15] L. Dubau, C. Coutanceau, E. Garnier, J.-M. Léger, C. Lamy, *J. Appl. Electrochem.* **2003**, *33*, 419. doi:10.1023/A:1024491007321
- [16] R. Raja, T. Khimyak, J. M. Thomas, S. Hermans, B. F. G. Johnson, *Angew. Chem. Int. Edit.* **2001**, *40*, 4638. doi:10.1002/1521-3773(20011217)40:24<4638::AID-ANIE4638>3.0.CO;2-W
- [17] R. D. Adams, T. S. Bamard, Z. Li, W. Wu, J. H. Yamamoto, *J. Am. Chem. Soc.* **1994**, *116*, 9103. doi:10.1021/JA00099A028
- [18] W. L. F. Armarego, C. L. L. Chai, *Purification of Laboratory Chemicals* **2003**, 5th edition (Butterworth-Heinemann: Bodmin, Cornwall).